Smart Mater. Struct. **18** (2009) 095040 (9pp) doi:10.1088/0964-1726/18/9/095040

An investigation on electromechanical stability of dielectric elastomers undergoing large deformation

Yanju Liu[1,3], Liwu Liu[1], Kai Yu[2], Shouhua Sun[1] and Jinsong Leng[2,3]

[1] Department of Astronautical Science and Mechanics, Harbin Institute of Technology (HIT), No. 92 West dazhi Street, PO Box 301, Harbin, 150001, Peoples Republic of China
[2] Centre for Composite Materials, Science Park of Harbin Institute of Technology (HIT), No. 2 YiKuang Street, PO Box 3011, Harbin, 150001, Peoples Republic of China

E-mail: yj_liu@hit.edu.cn and lengjs@hit.edu.cn

Received 11 May 2009, in final form 25 June 2009
Published 10 August 2009
Online at stacks.iop.org/SMS/18/095040

Abstract
Dielectric elastomers are one of the important electroactive polymers used as actuators in adaptive structures due to their outstanding ability to generate very large deformations when subjected to an external electric field. In this paper, the Mooney–Rivlin elastic strain energy function with two material constants is used to analyze the electromechanical stability performance of a dielectric elastomer. This elastic strain energy together with the electric energy incorporating linear permittivity are the main items to construct the free energy of the system. Particular numerical results are also calculated for a further understanding of the dielectric elastomer's typical stability performance. The proposed model offers great help in guiding the design and fabrication of actuators featuring dielectric elastomers.

(Some figures in this article are in colour only in the electronic version)

1. Introduction

Dielectric elastomers are widely used to fabricate actuators, sensors etc, due to their perfect properties of large deformation (up to 380%), high elastic energy density (3.4 J g^{-1}), high efficiency, high responsive speed, as well as long fatigue lifespan [1–12]. When a voltage is imposed on the dielectric elastomer film, the film will become thinner [13–20]. As a result, the actual electric field experienced by the dielectric elastomer becomes stronger at the same voltage, thus causing further thinning of the film thickness. The above process will continue. When the electric field exceeds the breakdown electric field, the dielectric elastomer will break down. This is called the electromechanical instability, or pull-in instability, which is the main reason preventing dielectric elastomers from being used in practical applications [21–26].

In recent years, the stability analysis of dielectric elastomers has become a most popular issue, especially after Suo *et al* proposed the electromechanical stability theory of dielectric elastomers [27–34]. In their published paper, Suo *et al* indicated that any free energy function can be used to analyze the electromechanical stability of a dielectric elastomer [27, 28]. For example, they used the elastic strain energy function with one material constant to analyze the stability of an ideal dielectric elastomer subjected to a biaxial stress. The results revealed the relation between the nominal electric displacement and the nominal electric field. It was the first time that the experimental phenomenon that pre-stretching could enhance the dielectric elastomer's stability had been proved theoretically. Meanwhile, the critical breakdown electric field strength has been predicted by using this method. Norrisa *et al* used the Ogden elastic strain energy model to analyze the dielectric elastomer's stability [33]. The relation among critical actual electric field, nominal stress and the pre-stretching ratio of dielectric elastomers was accurately obtained. Simultaneously, as a particular case, a neo-hookean model, which was a simplified model of the Ogden model, was introduced to give more concise and accurate results. Further research was done on the stability of neo-hookean silicone based elastomer by Díaz-Calleja's group [34]. The

[3] Authors to whom any correspondence should be addressed.

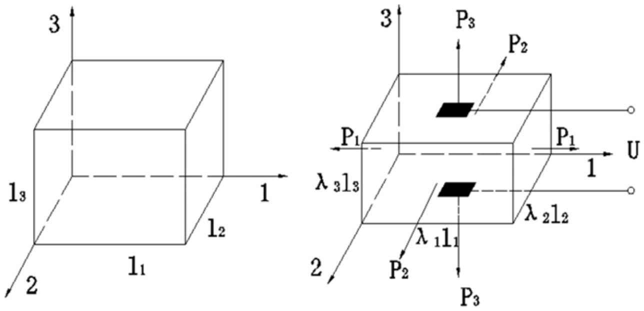

Figure 1. Dielectric elastomer electromechanical coupling system. λ_1, λ_2 denote the in-plane principal stretch ratios of the dielectric elastomer, λ_3 is the stretch ratio of the dielectric elastomer thickness direction, l_1, l_2, l_3 are the original dimensions of the dielectric elastomer, P_1, P_2, P_3 denote the pre-stretch forces, subject to mechanical forces in three directions, and to an electrical voltage U via an external circuit, that deforms to $\lambda_1 l_1$, $\lambda_2 l_2$, $\lambda_3 l_3$.

Hessian matrix under two special loading conditions was deduced. Furthermore, the stable and unstable domains of dielectric elastomers were determined. These results can help us understand the stability performance of neo-hookean silicone more thoroughly. An elastic strain energy function with two material constants was used to analyze the stability performance of dielectric elastomers by our group. The introduction of a material constant ratio k offers great help in analyzing the stability of various dielectric elastomers [32]. The relationship between the nominal electric displacement and nominal electric field of different dielectric elastomers is derived directly by using this model.

In the current work, differently from that given in Suo's paper [31], the system free energy containing the Mooney–Rivlin elastic strain energy function with two material constants and an electric energy incorporating linear permittivity has been constructed to analyze the electromechanical stability of a dielectric elastomer. The proposed model is helpful in guiding the design and fabrication of dielectric elastomer based devices.

2. The basic theory

For a dielectric elastomer, the permittivity is a variable which depends on the macromolecular structure, crosslink degree and pre-stretching of the elastomer. This has already been proved by theoretical and experimental research. Suo *et al* indicated that if the crosslink degree is high, or if the deformation approaches the extension limit, the permittivity of the dielectric elastomer will be affected by its deformation. Therefore, due to the fact that the dielectric elastomer will experience a nonlinear large deformation under the coupled mechanical and electric field, it is necessary to introduce a variable dielectric permittivity into the dielectric energy when analyzing the elastomer's stability performance.

In their recently published paper [31], Suo *et al* used a dielectric permittivity which is a linear fitted function of experimental data in analyzing the mechanical behavior and stability of a dielectric elastomer undergoing a large deformation. Based on their research, the expression of permittivity $\varepsilon(\lambda_1, \lambda_2, \lambda_3)$ is expressed as:

$$\varepsilon(\lambda_1, \lambda_2, \lambda_3) = [1 + a(\lambda_3 - 1) + b(\lambda_1 + \lambda_2 + \lambda_3 - 3)]\varepsilon^{\sim} \quad (1)$$

where $\varepsilon^{\sim}$ is the permittivity of the dielectric elastomer without deformation, a and b are the coefficients of electrostriction. λ_i $(i = 1, 2, 3)$ are stretch ratios, λ_1 and λ_2 denote the in-plane principal stretch ratios of the dielectric elastomer film (perpendicular to the electric field), λ_3 is the stretch ratio along the direction of the electric field, as shown in figure 1.

The free energy function of the dielectric elastomer electromechanical coupling system can be written as [27–34, 36–39]:

$$W(\lambda_1, \lambda_2, \lambda_3, D^{\sim}) = U(\lambda_1, \lambda_2, \lambda_3) + V(\lambda_1, \lambda_2, \lambda_3, D^{\sim}) \quad (2)$$

where $W(\lambda_1, \lambda_2, \lambda_3, D^{\sim})$ represents the system free energy function, $U(\lambda_1, \lambda_2, \lambda_3)$ denotes the elastic strain energy density function, $V(\lambda_1, \lambda_2, \lambda_3, D^{\sim})$ is the electric energy density function, and $D^{\sim}$ is the nominal electric displacement of the electromechanical coupling system.

The electric energy density function of a dielectric elastomer with a linear permittivity can be expressed as follows [31]:

$$V(\lambda_1, \lambda_2, \lambda_3, D^{\sim}) = \frac{D^{\sim 2}}{2\varepsilon(\lambda_1, \lambda_2, \lambda_3)}\lambda_1^{-1}\lambda_2^{-1}\lambda_3. \quad (3)$$

The nominal stress s_i and the nominal electric field $E^{\sim}$ depend on the following functions respectively:

$$s_i = \frac{\partial W(\lambda_1, \lambda_2, \lambda_3, D^{\sim})}{\partial \lambda_i} \quad (4)$$

$$E^{\sim} = \frac{\partial W(\lambda_1, \lambda_2, \lambda_3, D^{\sim})}{\partial D^{\sim}}. \quad (5)$$

The Mooney–Rivlin model of the elastic strain energy function with two material constants is given by [33]:

$$U(\lambda_1, \lambda_2, \lambda_3) = \frac{C_1}{2}(\lambda_1^2 + \lambda_2^2 + \lambda_3^2 - 3) + \frac{C_2}{2}(\lambda_1^{-2} + \lambda_2^{-2} + \lambda_3^{-2} - 3) \quad (6)$$

where C_1 and C_2 are two material constants, which can be determined by experiment. Under the condition of constant permittivity of the electric energy density function, the effect of the free energy function on the dielectric elastomer stability performance was studied in our previously published work [32]. Based on this, if $C_2 = 0$, the above equation is the elastic strain energy used by Suo *et al* in system stability analysis of the dielectric elastomer [27].

Substituting equations (6), (1), (3) and (2) into (4) and (5), the nominal stress and the nominal electric field can be expressed respectively as follows:

$$s_1 = C_1\lambda_1 - C_2\lambda_1^{-3} - \frac{\lambda_1^{-2}\lambda_2^{-1}\lambda_3 D^{\sim 2}}{2[1 + a(\lambda_3 - 1) + b(\lambda_1 + \lambda_2 + \lambda_3 - 3)]\varepsilon^{\sim}} - \frac{b\lambda_1^{-1}\lambda_2^{-1}\lambda_3 D^{\sim 2}}{2[1 + a(\lambda_3 - 1) + b(\lambda_1 + \lambda_2 + \lambda_3 - 3)]^2\varepsilon^{\sim}} \quad (7)$$

$$s_2 = C_1\lambda_2 - C_2\lambda_2^{-3} - \frac{\lambda_1^{-1}\lambda_2^{-2}\lambda_3 D^{\sim 2}}{2[1+a(\lambda_3-1)+b(\lambda_1+\lambda_2+\lambda_3-3)]\varepsilon^{\sim}} - \frac{b\lambda_1^{-1}\lambda_2^{-1}\lambda_3 D^{\sim 2}}{2[1+a(\lambda_3-1)+b(\lambda_1+\lambda_2+\lambda_3-3)]^2\varepsilon^{\sim}} \quad (8)$$

$$s_3 = C_1\lambda_3 - C_2\lambda_3^{-3} + \frac{\lambda_1^{-1}\lambda_2^{-1} D^{\sim 2}}{2[1+a(\lambda_3-1)+b(\lambda_1+\lambda_2+\lambda_3-3)]\varepsilon^{\sim}} - \frac{(a+b)\lambda_1^{-1}\lambda_2^{-1}\lambda_3 D^{\sim 2}}{2[1+a(\lambda_3-1)+b(\lambda_1+\lambda_2+\lambda_3-3)]^2\varepsilon^{\sim}} \quad (9)$$

$$E^{\sim} = \frac{\lambda_1^{-1}\lambda_2^{-1}\lambda_3 D^{\sim}}{[1+a(\lambda_3-1)+b(\lambda_1+\lambda_2+\lambda_3-3)]\varepsilon^{\sim}}. \quad (10)$$

As shown in figure 1, the original dimensions of the dielectric elastomer in the three main directions are denoted as l_i in the original state, prior to deformation. When applying an external load P_i in the three main directions, the dimensions of the dielectric elastomer become L_i. Therefore, the stretch ratios in the main directions are defined as $\lambda_i = L_i/l_i$, Furthermore, the nominal stresses in the main directions can be expressed as: $s_1 = P_1/l_2l_3$, $s_2 = P_2/l_1l_3$, $s_3 = P_3/l_1l_2$. The corresponding real stresses can be expressed as: $\sigma_1 = P_1/L_2L_3$, $\sigma_2 = P_2/L_1L_3$, $\sigma_3 = P_3/L_1L_2$. Thus, based on the above given relationship, the real stresses can be written as: $\sigma_1 = s_1/\lambda_2\lambda_3$, $\sigma_2 = s_2/\lambda_1\lambda_3$, $\sigma_3 = s_3/\lambda_1\lambda_2$. Substituting them into equations (7), (8) and (9), we then have:

$$\sigma_1 = (C_1\lambda_1 - C_2\lambda_1^{-3})\lambda_2^{-1}\lambda_3^{-1} - \frac{\lambda_1^{-2}\lambda_2^{-2} D^{\sim 2}}{2[1+a(\lambda_3-1)+b(\lambda_1+\lambda_2+\lambda_3-3)]\varepsilon^{\sim}} - \frac{b\lambda_1^{-1}\lambda_2^{-2} D^{\sim 2}}{2[1+a(\lambda_3-1)+b(\lambda_1+\lambda_2+\lambda_3-3)]^2\varepsilon^{\sim}} \quad (11)$$

$$\sigma_2 = (C_1\lambda_2 - C_2\lambda_2^{-3})\lambda_1^{-1}\lambda_3^{-1} - \frac{\lambda_1^{-2}\lambda_2^{-2} D^{\sim 2}}{2[1+a(\lambda_3-1)+b(\lambda_1+\lambda_2+\lambda_3-3)]\varepsilon^{\sim}} - \frac{b\lambda_1^{-2}\lambda_2^{-1} D^{\sim 2}}{2[1+a(\lambda_3-1)+b(\lambda_1+\lambda_2+\lambda_3-3)]^2\varepsilon^{\sim}} \quad (12)$$

$$\sigma_3 = (C_1\lambda_3 - C_2\lambda_3^{-3})\lambda_1^{-1}\lambda_2^{-1} + \frac{\lambda_1^{-2}\lambda_2^{-2} D^{\sim 2}}{2[1+a(\lambda_3-1)+b(\lambda_1+\lambda_2+\lambda_3-3)]\varepsilon^{\sim}} - \frac{(a+b)\lambda_1^{-2}\lambda_2^{-2}\lambda_3 D^{\sim 2}}{2[1+a(\lambda_3-1)+b(\lambda_1+\lambda_2+\lambda_3-3)]^2\varepsilon^{\sim}} \quad (13)$$

$$E = \frac{D}{[1+a(\lambda_3-1)+b(\lambda_1+\lambda_2+\lambda_3-3)]\varepsilon^{\sim}}. \quad (14)$$

Substituting equations (14) into (11)–(13), since $D = D^{\sim}\lambda_1^{-1}\lambda_2^{-1}$, the item $\lambda_1^{-2}\lambda_2^{-2}D^{\sim 2}/2[1+a(\lambda_3-1)+b(\lambda_1+\lambda_2+\lambda_3-3)]\varepsilon^{\sim}$ in equations (11)–(13) becomes $\varepsilon^{\sim}E^2/2$, the item $b\lambda_1^{-1}\lambda_2^{-2}D^{\sim 2}/2[1+a(\lambda_3-1)+b(\lambda_1+\lambda_2+\lambda_3-3)]^2\varepsilon^{\sim}$ in equations (11) becomes $\frac{\partial\varepsilon}{2\partial\lambda_1}\lambda_1 E^2$, the third term in equations (12) and (13) becomes $\frac{\partial\varepsilon}{2\partial\lambda_2}\lambda_2 E^2$ $\frac{\partial\varepsilon}{2\partial\lambda_3}\lambda_3 E^2$ respectively. If the stretching rate is fixed, equation (14) denotes the linear relationship between the real electric displacement and the real electric field. Since equations (11)–(13) have similar expressions only equation (11) will be discussed in detail in the following part. On the right-hand side of equation (11), the first item is related to the elasticity, the second item represents the Maxwell stress, whose direction is the same as that of the imposed electric field, the third term is present when the permittivity of the dielectric elastomer varies with the stretch, and can be either tensile or compressive.

3. Incompressible dielectric elastomer

Supposing that the dielectric elastomer is incompressible, namely $\lambda_1\lambda_2\lambda_3 = 1$, according to Suo's theory [31], the nominal stress and the nominal electric field can be simplified as follows:

$$s_1 - \frac{s_3}{\lambda_1^2\lambda_2} = \frac{\partial W(\lambda_1,\lambda_2,D^{\sim})}{\partial\lambda_1} \quad (15)$$

$$s_2 - \frac{s_3}{\lambda_2^2\lambda_1} = \frac{\partial W(\lambda_1,\lambda_2,D^{\sim})}{\partial\lambda_2} \quad (16)$$

$$E^{\sim} = \frac{\partial W(\lambda_1,\lambda_2,D^{\sim})}{\partial D^{\sim}}. \quad (17)$$

Then the Mooney–Rivlin model can be simplified as well:

$$U(\lambda_1,\lambda_2) = \frac{C_1}{2}(\lambda_1^2+\lambda_2^2+\lambda_1^{-2}\lambda_2^{-2}-3) + \frac{C_2}{2}(\lambda_1^{-2}+\lambda_2^{-2}+\lambda_1^2\lambda_2^2-3). \quad (18)$$

Because the dielectric elastomer is incompressible, the permittivity can be simplified to a function of two stretch ratios in the two planar directions. Simplifying equation (1) the relationship between the permittivity and the stretch ratio of the dielectric elastomer film is:

$$\varepsilon(\lambda_1,\lambda_2) = [1+a(\lambda_1^{-1}\lambda_2^{-1}-1)+b(\lambda_1+\lambda_2+\lambda_1^{-1}\lambda_2^{-1}-3)]\varepsilon^{\sim} \quad (19)$$

where a, b are the electrostrictive coefficients of the dielectric elastomer.

When importing a non-dimensional factor, assuming $b = na$ in equation (19), n is defined as the electrical stretching coefficient ratio, which is related to both the dielectric elastomer and the load of the coupled field. Then, we consider conducting a dual axis stretch, that is $\lambda_1 = \lambda_2$. Based on Pelrine's experiment that the dielectric constant is dependent on the stretching ratio [35], we set $n = 1$, and the electrostrictive coefficient $a = -0.034$. When $n = 2, a = -0.01$. When $n = 3$, $a = -0.0058$. When $n = 4$, $a = -0.004$. With an increase of the stretching coefficient ratio n, the stretching coefficient increases.

Clearly, the range of electrostrictive coefficient a decreases along with an increase of deformation. For example, if $a = -1$, in order to satisfy the condition of a positive permittivity, the maximum value of the stretch rate should not exceed 1.62. Under this condition, the stretch rate does not reach its real critical value (In most cases, the pre-stretching ratio $\lambda^{\mathrm{p}} = 1.3$, the critical stretching ratio $\lambda^{\mathrm{C}} = 1.26$, the real critical value $\lambda_r^C = \lambda^p \lambda_C = 1.638$.). This can be thought of as the reason for the suppression of the instability performance. Generally, when the electrostrictive coefficient a satisfies $a < [(\frac{\varepsilon(\lambda_1,\lambda_2)}{\varepsilon^\sim} - 1)_{\lambda_r^C}]/[(n+1)(\lambda_r^C)^{-2} + 2n\lambda_r^C - (3n+1)]$, the instability performance of the dielectric elastomer is suppressed, where λ_C is the critical stretch rate of the dielectric elastomer and λ^p is the pre-stretch rate of the dielectric elastomer.

Then the system free energy function of the dielectric elastomer can be simplified as follows:

$$W(\lambda_1, \lambda_2, D^\sim) = \frac{C_1}{2}(\lambda_1^2 + \lambda_2^2 + \lambda_1^{-2}\lambda_2^{-2} - 3) + \frac{C_2}{2}(\lambda_1^{-2} + \lambda_2^{-2} + \lambda_1^2\lambda_2^2 - 3) + \frac{\lambda_1^{-2}\lambda_2^{-2}D^{\sim 2}}{2[1+a(\lambda_1^{-1}\lambda_2^{-1} - 1) + b(\lambda_1 + \lambda_2 + \lambda_1^{-1}\lambda_2^{-1} - 3)]\varepsilon^\sim}. \tag{20}$$

Substituting equation (20) into (11)–(13), the nominal stress and the nominal electric field of the dielectric elastomer electromechanical coupling system can be expressed as:

$$s_1 = C_1(\lambda_1 - \lambda_1^{-3}\lambda_2^{-2}) + C_2(-\lambda_1^{-3} + \lambda_1\lambda_2^2) - \frac{\lambda_1^{-3}\lambda_2^{-2}D^{\sim 2}}{[1 + a(\lambda_1^{-1}\lambda_2^{-1} - 1) + b(\lambda_1 + \lambda_2 + \lambda_1^{-1}\lambda_2^{-1} - 3)]\varepsilon^\sim} - \frac{[b-(b+a)\lambda_1^{-2}\lambda_2^{-1}]\lambda_1^{-2}\lambda_2^{-2}D^{\sim 2}}{2[1 + a(\lambda_1^{-1}\lambda_2^{-1} - 1) + b(\lambda_1 + \lambda_2 + \lambda_1^{-1}\lambda_2^{-1} - 3)]^2\varepsilon^\sim} \tag{21}$$

$$s_2 = C_1(\lambda_2 - \lambda_2^{-3}\lambda_1^{-2}) + C_2(-\lambda_2^{-3} + \lambda_2\lambda_1^2) - \frac{\lambda_1^{-2}\lambda_2^{-3}D^{\sim 2}}{[1 + a(\lambda_1^{-1}\lambda_2^{-1} - 1) + b(\lambda_1 + \lambda_2 + \lambda_1^{-1}\lambda_2^{-1} - 3)]\varepsilon^\sim} - \frac{[b-(b+a)\lambda_1^{-1}\lambda_2^{-2}]\lambda_1^{-2}\lambda_2^{-2}D^{\sim 2}}{2[1 + a(\lambda_1^{-1}\lambda_2^{-1} - 1) + b(\lambda_1 + \lambda_2 + \lambda_1^{-1}\lambda_2^{-1} - 3)]^2\varepsilon^\sim} \tag{22}$$

$$E^\sim = \frac{\lambda_1^{-2}\lambda_2^{-2}D^\sim}{[1 + a(\lambda_1^{-1}\lambda_2^{-1} - 1) + b(\lambda_1 + \lambda_2 + \lambda_1^{-1}\lambda_2^{-1} - 3)]\varepsilon^\sim}. \tag{23}$$

The real stress and real electric field of the dielectric elastomer can be expressed as:

$$\sigma_1 = C_1(\lambda_1^2 - \lambda_1^{-2}\lambda_2^{-2}) + C_2(\lambda_1^2\lambda_2^2 - \lambda_1^{-2}) - \varepsilon E^2 - \frac{\varepsilon^\sim[b\lambda_1 - (b+a)\lambda_1^{-1}\lambda_2^{-1}]}{2}E^2 \tag{24}$$

$$\sigma_2 = C_1(\lambda_2^2 - \lambda_1^{-2}\lambda_2^{-2}) + C_2(\lambda_1^2\lambda_2^2 - \lambda_2^{-2}) - \varepsilon E^2 - \frac{\varepsilon^\sim[b\lambda_2 - (b+a)\lambda_1^{-1}\lambda_2^{-1}]}{2}E^2 \tag{25}$$

$$E = \frac{D}{[1 + a(\lambda_1^{-1}\lambda_2^{-1} - 1) + b(\lambda_1 + \lambda_2 + \lambda_1^{-1}\lambda_2^{-1} - 3)]\varepsilon^\sim}. \tag{26}$$

According to the well-known working principle of dielectric elastomer actuators, the area of the dielectric elastomer film is enlarged, accompanied by a related thickness reduction, under the stimulation of both the mechanical load and the electric field. This performance increases the inner electric field of the dielectric elastomer. When the electric field reaches the critical value, the film is broken down; this is called the instability of the system. Apparently, the effect of the mechanical stress field acting on the electromechanical coupling system is characterized by the elastic strain energy function, while the electric energy density function characterizes the effect of the electric field. According to the methods developed, the following research is focused on the effect of deformation based permittivity on the dielectric elastomer electromechanical stability performance [31].

4. Stability analysis

In the first loading case, we suppose the in-plane stretch of the dielectric elastomer is biaxial and $\lambda_1 = \lambda_2 = \lambda$. Due to the dielectric elastomer's incompressibility, we have $\lambda_3 = \lambda^{-2}$, and then the free energy function can be written as:

$$W(\lambda, D^\sim) = \frac{C_1}{2}(2\lambda^2 + \lambda^{-4} - 3) + \frac{C_2}{2}(2\lambda^{-2} + \lambda^4 - 3) + \frac{\lambda^{-4}D^{\sim 2}}{2[1 + a(\lambda^{-2} - 1) + b(2\lambda + \lambda^{-2} - 3)]\varepsilon^\sim}. \tag{27}$$

Introducing a dimensionless quantity k, which depends on the material and the activated shape, simultaneously set $C_2 = kC_1$, where C_1 is a constant, as $k = 0$, $C_2 = 0$. The system free energy function is changed to Suo's form [32]. Considering the non-dimensional coefficient n, $b = na$. To get the relationship between nominal electric displacement and nominal electric field, stretch ratio and nominal electric field, respectively, let $s_1(\lambda, D^\sim) = 0$. Furthermore we have $\partial W(\lambda, D^\sim)/\partial\lambda = 0$. Substituting equation (27) into it, we have:

$$\frac{D^\sim}{\sqrt{C_1\varepsilon^\sim}} = \{\{2[(\lambda^6 - 1) + k(\lambda^8 - \lambda^2)]\}\{2 + a\lambda[n - (n+1)\lambda^{-3}] \times \{1 + a[2n\lambda + (n+1)\lambda^{-2} - (3n+1)]\}^{-1}\}^{-1} \times \{1 + a[2n\lambda + (n+1)\lambda^{-2} - (3n+1)]\}\}^{1/2} \tag{28}$$

$$\frac{E^\sim}{\sqrt{C_1/\varepsilon^\sim}} = \frac{\lambda^{-4}}{1 + a(\lambda^{-2} - 1) + b(2\lambda + \lambda^{-2} - 3)} \times \frac{D^\sim}{\sqrt{C_1\varepsilon^\sim}} \tag{29}$$

$$\frac{E^\sim}{\sqrt{C_1/\varepsilon^\sim}} = \{\{2[(\lambda^{-2} - \lambda^{-8}) + k(1 - \lambda^{-6})]\} \times \{2 + a\lambda[n - (n+1)\lambda^{-3}] \times \{1 + a[2n\lambda + (n+1)\lambda^{-2} - (3n+1)]\}^{-1}\}^{-1} \times \{1 + a[2n\lambda + (n+1)\lambda^{-2} - (3n+1)]\}^{-1}\}^{1/2}. \tag{30}$$

Figure 2 illustrates the stability performance of different dielectric elastomer materials under the loading condition as λ_1 and $n = 1$, Figures 2(a)–(d) show the relationship between the nominal electric displacement and the nominal electric field of the dielectric elastomer with different values of k (1, 1/2, 1/4 and 1/5) [32] and different values of a (−1, −0.04, −0.034, 0.04) respectively. Evidently, along with the decrease of a, the peaks of the nominal electric field decrease. However, the comparative stability performance of such a kind of dielectric

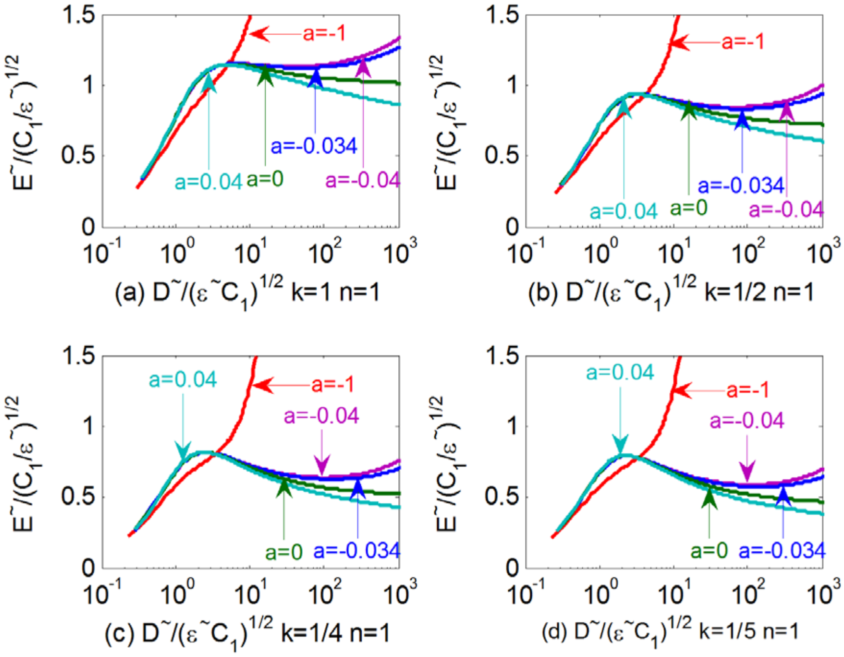

Figure 2. Relationship between the nominal electric displacement and the nominal electric field of dielectric elastomers for various values of r and k, under stretches that are biaxially equal $\lambda_1 = \lambda_2 = \lambda$ (a) $k = 1$, (b) $k = 1/2$, (c) $k = 1/4$, (d) $k = 1/5$.

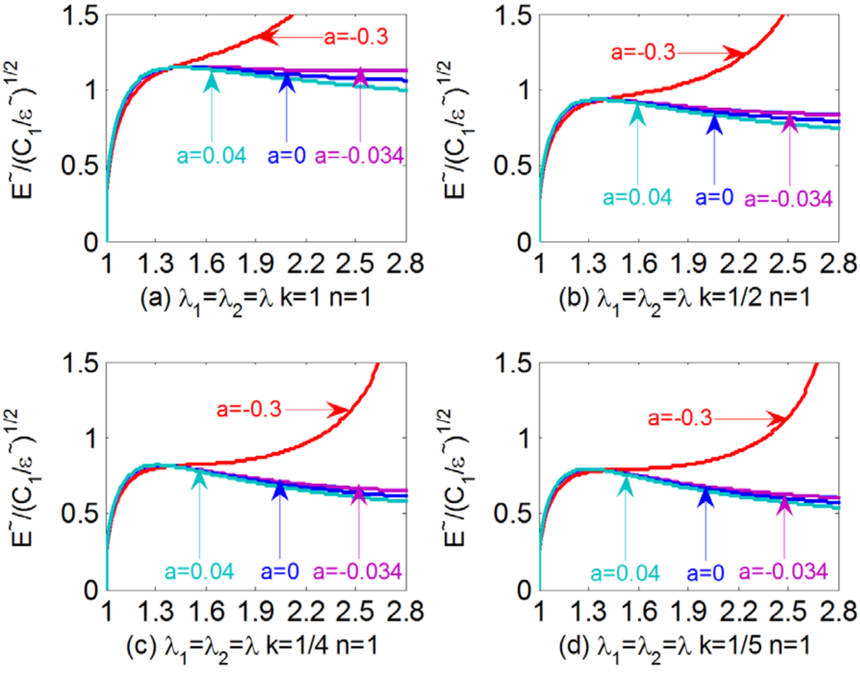

Figure 3. Relationship between the stretch ratio and the nominal electric field of different dielectric elastomers with different values of r and k, under stretches that are biaxially equal $\lambda_1 = \lambda_2 = \lambda$ (a) $k = 1$, (b) $k = 1/2$, (c) $k = 1/4$, (d) $k = 1/5$.

elastomer is even lower. When $a = 0$, neglecting the effect of deformation on the dielectric elastomer permittivity, it degenerates to the analysis of an ideal dielectric elastomer [32]. For example, when $k = 1/2$, the nominal electric field peak $E^{\sim}_{\max} = 0.9363\sqrt{C_1/\varepsilon^{\sim}}$, but considering a special value of a, namely $a = -0.034$, if k takes different values of 1, 1/2, 1/4 and 1/5 respectively, the corresponding nominal electric field peaks are $1.1521\sqrt{C_1/\varepsilon^{\sim}}$, $0.9361\sqrt{C_1/\varepsilon^{\sim}}$, $0.8158\sqrt{C_1/\varepsilon^{\sim}}$, $0.7905\sqrt{C_1/\varepsilon^{\sim}}$ respectively.

Figure 3 illustrates the relationship between the stretch ratio and the nominal electric field of different dielectric elastomers under a biaxial stretch with $\lambda_1 = \lambda_2 = \lambda$. Taking, as a special example, various values of k are selected, namely $k = 1, 1/2, 1/4, 1/5$. When $k = 1/2$, $a = 0$ and

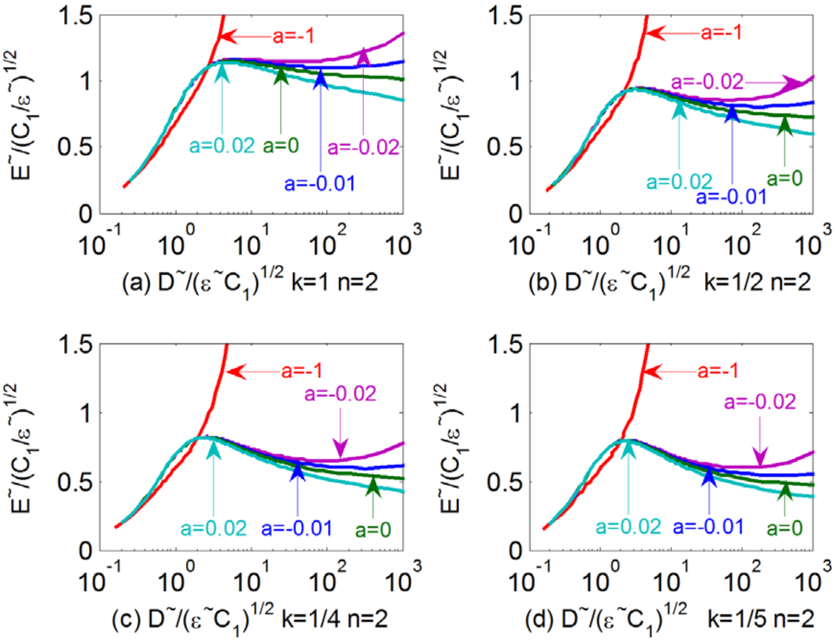

Figure 4. Relationship between the nominal electric displacement and the nominal electric field of dielectric elastomers for various values of r and k, under stretches that are biaxially equal $\lambda_3 = \lambda$ (a) $k = 1$, (b) $k = 1/2$, (c) $k = 1/4$, (d) $k = 1/5$.

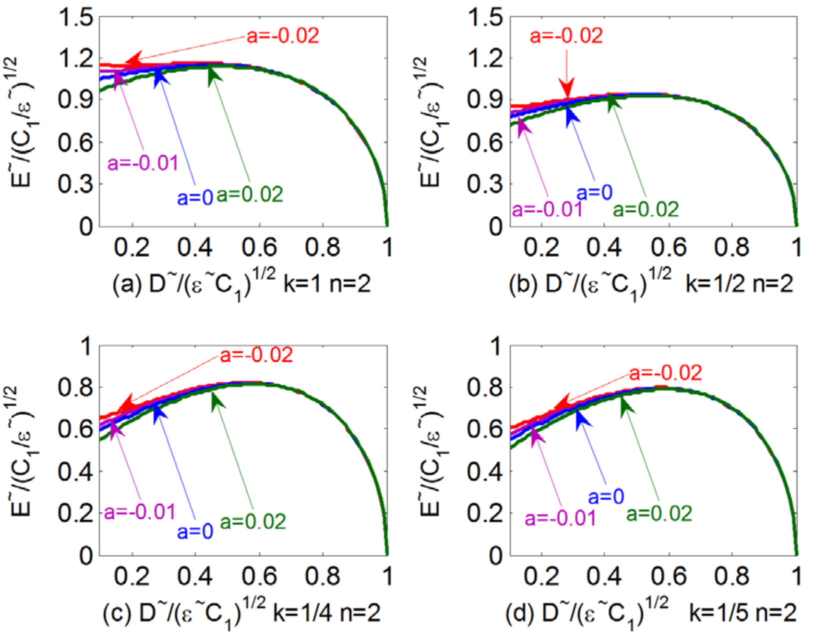

Figure 5. Relationship between the stretch ratio and the nominal electric field of different dielectric elastomers with different values of r and k, $\lambda_3 = \lambda$ (a) $k = 1$, (b) $k = 1/2$, (c) $k = 1/4$, (d) $k = 1/5$.

the nominal electric field reaches its peak, the corresponding stretch ratio (the critical value) $\lambda^C = 1.37$, which is consistent with the conclusion based on [32]. In the same condition, if a takes different values (-0.04, -0.034, 0.04), when the nominal electric field reaches its peak, the corresponding critical stretch ratios are $\lambda^C = 1.36$, $\lambda^C = 1.39$, $\lambda^C = 1.40$ respectively. Evidently, all the results are consistent with Suo's conclusion [28].

In a second special case, we take the stretching perpendicular to the elastomer film as $\lambda_3 = \lambda$. Owing to the incompressibility condition of the dielectric elastomer, we have $\lambda_1 = \lambda_2 = \lambda^{-1/2}$, then the free energy function can be expressed as follows:

$$W(\lambda, D^{\sim}) = \frac{C_1}{2}(\lambda^2 + 2\lambda^{-1} - 3) + \frac{C_2}{2}(\lambda^{-2} + 2\lambda - 3) + \frac{\lambda^2 D^{\sim 2}}{2[1 + a(\lambda - 1) + b(2\lambda^{-1/2} + \lambda - 3)]\varepsilon^{\sim}}. \quad (31)$$

Similarly, let $s_1(\lambda, D^{\sim}) = 0$, furthermore we have $\partial W(\lambda, D^{\sim})/\partial\lambda = 0$. Substituting equation (24) into it, then

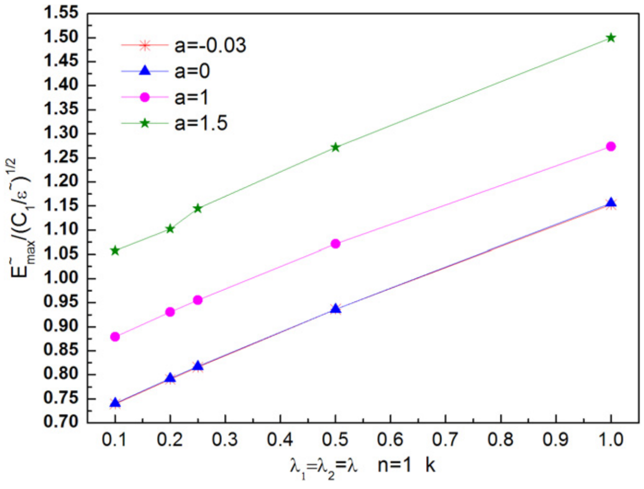

Figure 6. The critical nominal electric field when electrostriction coefficient r takes different values under the loading condition $\lambda_1 = \lambda_2 = \lambda$.

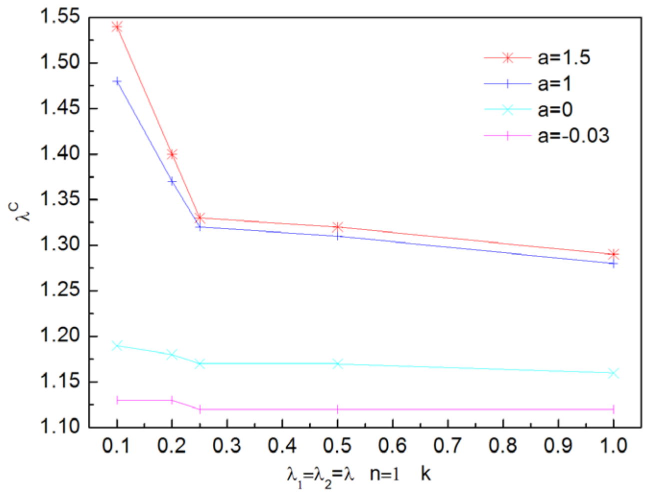

Figure 7. The critical stretch ratio when electrostriction coefficient r takes different values under the loading condition $\lambda_1 = \lambda_2 = \lambda$.

we have:

$$\frac{D^{\sim}}{\sqrt{C_1\varepsilon^{\sim}}} = \{\{2[(\lambda^{-2} - \lambda) + k(\lambda^{-3} - 1)]\} \times \{2\lambda - a\lambda^2(1 + n - n\lambda^{-3/2}) \times \{1 + a[2n\lambda^{-12} + (n+1)\lambda - (3n+1)]\}^{-1}\}^{-1} \times \{1 + a[2n\lambda^{-1/2} + (n+1)\lambda - (3n+1)]\}\}^{1/2} \quad (32)$$

$$\frac{E^{\sim}}{\sqrt{C_1/\varepsilon^{\sim}}} = \frac{\lambda^2}{1 + a(\lambda - 1) + b(2\lambda^{-1/2} + \lambda - 1)} \times \frac{D^{\sim}}{\sqrt{C_1\varepsilon^{\sim}}} \quad (33)$$

$$\frac{E^{\sim}}{\sqrt{C_1/\varepsilon^{\sim}}} = \{\{2[(\lambda^2 - \lambda^5) + k(\lambda - \lambda^4)]\} \times \{2\lambda - a\lambda^2(1 + n - n\lambda^{-3/2}) \times \{1 + a[2n\lambda^{-1/2} + (n+1)\lambda - (3n+1)]\}^{-1}\}^{-1} \times \{1 + a[2n\lambda^{-1/2} + (n+1)\lambda - (3n+1)]\}^{-1}\}^{1/2}. \quad (34)$$

Figure 4 illustrates the stability performance of different dielectric elastomer materials in a loading condition as $\lambda_3 = \lambda$ and $n = 2$. Figures 4(a)–(d) show the relationship between the nominal electric displacement and nominal electric field of the dielectric elastomer with different values of k (1, 1/2, 1/4 and 1/5) and different values of a (−1, −0.02, −0.01, 0 and 0.02) respectively. Evidently, with the decrease of a, or the increase of k, the critical electric field of the dielectric elastomer increases, and the dielectric elastomer becomes more stable. When $a = 0$, neglecting the influence of deformation on the dielectric elastomer's permittivity, it degenerates to the analysis of the ideal dielectric elastomer. For example, when $k = 1/5$, the nominal electric field peak is $E^{\sim}_{max} = 0.7923\sqrt{C_1/\varepsilon^{\sim}}$, this is consistent with the conclusions in our previous work [32]. On the other hand, let a take a special value $a = 0.02$, if k takes different values of 1, 1/2, 1/4 and 1/5, then the corresponding nominal electric field peaks are $E^{\sim}_{max} = 1.1367\sqrt{C_1/\varepsilon^{\sim}}$, $E^{\sim}_{max} = 0.9364\sqrt{C_1/\varepsilon^{\sim}}$, $E^{\sim}_{max} = 0.8138\sqrt{C_1/\varepsilon^{\sim}}$ and $E^{\sim}_{max} = 0.7892\sqrt{C_1/\varepsilon^{\sim}}$ respectively.

Figure 5 illustrates the relationship between the stretch ratio and the nominal electric field of different dielectric elastomers under the loading condition $\lambda_3 = \lambda$. By a similar method to that mentioned above, various values of k are selected, $k = 1, 1/2, 1/4, 1/5$. Taking as a special example ($k = 1/4$), if a takes different values (−0.02, −0.01, 0 and 0.02), when the nominal electric field reaches its peak, the corresponding critical stretch ratios are $\lambda^C = 0.58$, $\lambda^C = 0.57$, $\lambda^C = 0.57$ and $\lambda^C = 0.56$ respectively.

5. The critical nominal electric field, the critical stretch ratio, the critical area strain and the critical thickness strain

From stability to instability, the critical value of electromechanical coupling system is called the critical electric field of the dielectric elastomer. It is an important parameter in measuring the dielectric elastomer electromechanical coupling system stability level. The system stability gets higher along with an increase of the critical electric field. When the system reaches its critical electric field, the corresponding stretch rate is called the system critical stretch ratio. Under the state of stability, it is the maximum stretching deformation of an dielectric elastomer with the coupling of mechanical and electric fields. Similarly, the critical area strain and the critical thickness strain represent the maximum area and thickness deformation of the dielectric elastomer respectively.

In this section, the changing law of the parameters characterizing the elastomer's stability performance are discussed under two typical loading conditions as $\lambda_1 = \lambda_2 = \lambda$ and $\lambda_3 = \lambda$. Figures 6–9 show the changing laws of the critical nominal electric field, the critical stretch ratio, the critical area strain and the critical thickness strain by taking various parameters k as the variable while the deformation ratio a takes different values ($n = 1$). As shown in these figures, it is apparent that the critical nominal electric field, the critical stretch ratio, the critical area strain and the critical thickness strain all increase with an increase in parameter k. It

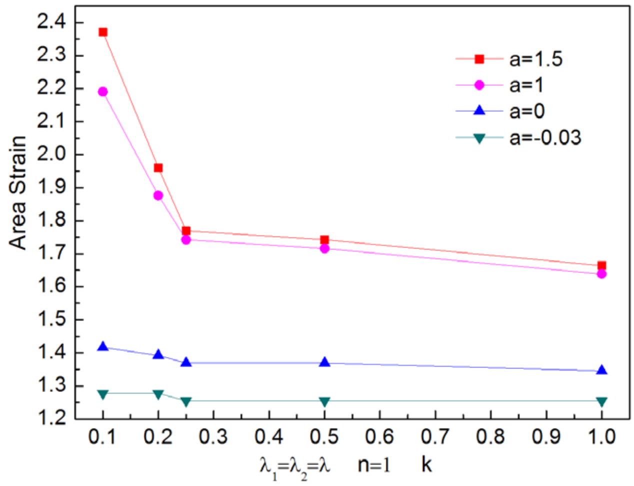

Figure 8. The critical area strain when the electrostriction coefficient r takes different values under the loading condition $\lambda_1 = \lambda_2 = \lambda$.

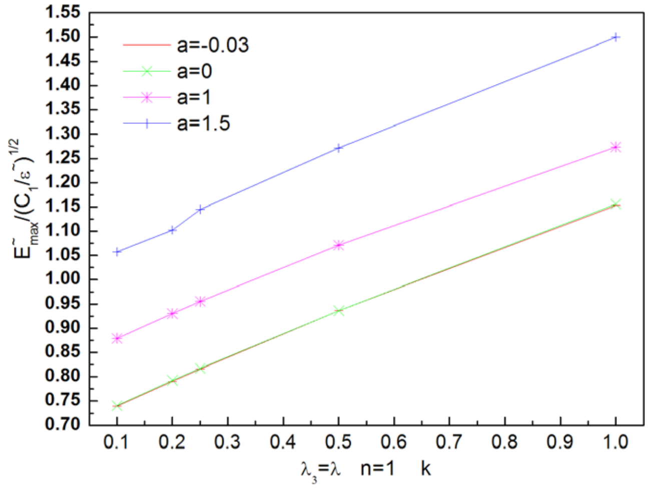

Figure 10. The critical nominal electric field when electrostriction coefficient r takes different values under the loading condition $\lambda_3 = \lambda$.

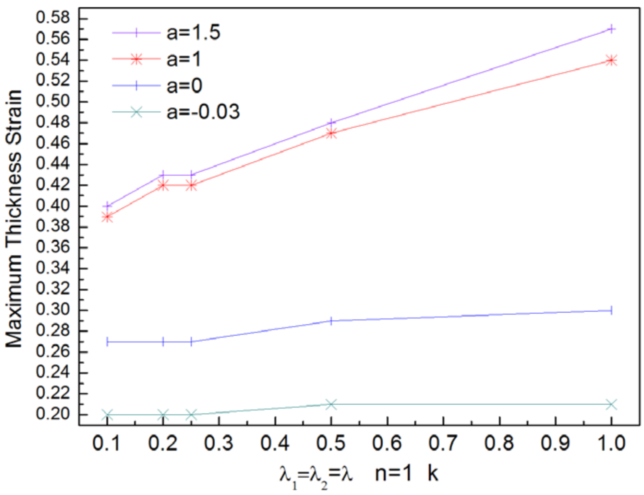

Figure 9. The critical thickness strain when electrostriction coefficient r takes different values under the loading condition $\lambda_1 = \lambda_2 = \lambda$.

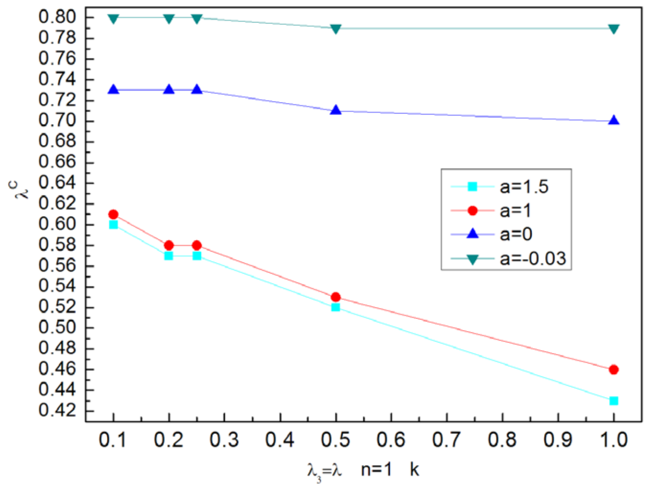

Figure 11. The critical stretch ratio when electrostriction coefficient r takes different values under the loading condition $\lambda_3 = \lambda$.

means that a electromechanical coupling system with higher k is more stable, and such system can approach its largest stretch ratio, largest area strain and largest thickness strain. All of these results are consistent with our previous conclusions. If the deformation ratio a increases, then the critical nominal electric field, the critical stretch ratio, the critical area strain and the critical thickness strain all increase. It means that a electromechanical coupling system with a higher a is more stable, and such system can tolerate a relatively larger stretch ratio, area strain and thickness strain.

Figures 10–13 show the changing laws of the critical nominal electric field, the critical stretch ratio, the critical area strain and the critical thickness strain by taking the material parameter k as a variable when deformation ratio a takes different values under a loading condition $\lambda_3 = \lambda$. Evidently, the critical nominal electric field, the critical area strain and the critical thickness strain increase with increasing k. At the same time, the critical stretch ratio decreases, this is due to the direction along thickness being the reference direction in this case. Similarly to the previous example, an electromechanical coupling system with a higher k is more stable. Furthermore, with increasing a, the critical nominal electric field, the critical area strain and the critical thickness strain increase but the critical stretching ratio decreases. It indicates that the higher a is, the more stable the electromechanical coupling system is.

From the above two examples, it can be concluded that to fabricate superior-performance dielectric elastomer based devices, dielectric elastomers materials with higher k and higher a would be better choices.

6. Conclusions

In this paper, the system free energy function, coupled by the elastic strain energy function with two material constants and an electric energy density function with a linear permittivity, is presented to analyze the electromechanical stability

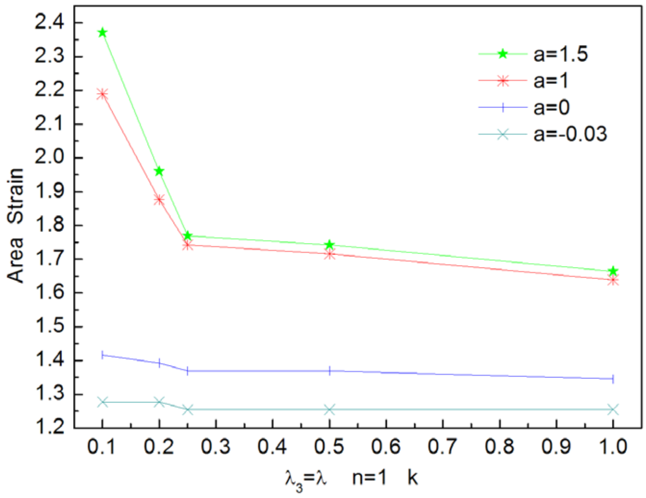

Figure 12. The critical area strain when the electrostriction coefficient *r* takes different values under the loading condition $\lambda_3 = \lambda$.

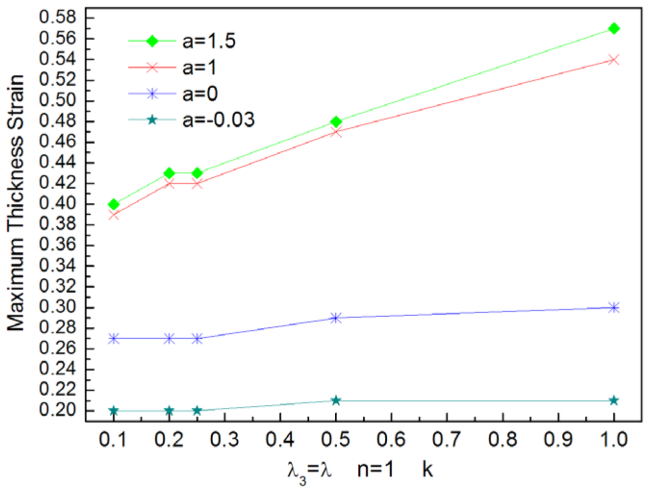

Figure 13. The critical thickness strain when electrostriction coefficient *r* takes different values under the loading condition $\lambda_3 = \lambda$.

performance of dielectric elastomers. The relationships among the stability parameters under two special loading conditions are also obtained. Along with the increase of the material constant ratio k, the nominal electric field peak, critical area strain and the critical thickness strain is higher. This indicates that the dielectric elastomer electromechanical system is more stable. Inversely, with an increase of the deformation coefficient a, the nominal electric field peak, critical area strain and the critical thickness strain increase, and the coupling system is more stable. The conclusions may be important in designing and fabricating superior-performance actuators based on dielectric elastomers.

Acknowledgments

This work is supported by plans for the development of high technology (863) and supported by Program for New Century Excellent Talents in University.

References

[1] Bar-Cohen Yseph 2001 *Electroactive Polymer (EAP) Actuators as Artificial Muscle: Reality, Potential and Challenges* (*SPIE Press Monograph* vol 482) (Bellingham, WA: SPIE Optical Engineering Press)
[2] Pelrine R, Kornbluh R, Pei Q B and Joseph J 2000 *Science* **287** 836
[3] Zhang Z, Liu L, Deng G, Sun S and Leng J 2009 *Proc. SPIE* **7287** 72871V
[4] Pelrine R E, Kornbluh R D and Joseph J P 1998 *Sensors Actuators* A **64** 77
[5] Plante J S and Dubowsky S 2007 *Smart Mater. Struct.* **16** S227
[6] Wissler M and Mazza E 2007 *Sensors Actuators* A **120** 185
[7] Kofod G, Paajanen M and Bauer S 2006 *Appl. Phys.* A **85** 141
[8] Gallone G, Carpi F, De Rossi D, Levita G and Marchetti A 2007 *Mater. Sci. Eng.* C **27** 110
[9] Carpi F and De Rossi D 2005 *IEEE Trans. Dielectr. Electr. Insul.* **12** 835
[10] Liu L, Fan J, Zhang Z, Shi L, Liu Y and Leng J 2008 *Adv. Mater. Res.* **47–50** 298
[11] Zhang Z, Liu L, Fan J, Yu K, Liu Y, Shi L and Leng J 2008 *Proc. SPIE* **6916** 691610
[12] Shi L, Liu Y, Liu L, Zhang Z and Leng J 2008 *Proc. SPIE* **6927** 69271A
[13] Liu L, Liu Y, Zhang Z, Yu K, Deng G, Sun S, Shi L and Leng J 2009 *Proc. SPIE* **7287** 728719
[14] Madden J D, Vandesteeg N, Madden P G, Takshi A, Zimet R, Anquetil P A, Lafontaine S R, Wierenga P A and Hunter I W 2004 *IEEE J. Ocean. Eng.* **29** 706
[15] Liu S F, Park S E, Cross L E and Shrout T R 2002 *J. Appl. Phys.* **92** 461
[16] Su J, Xu T B, Zhang S J, Shrout T R and Zhang Q M 2004 *Appl. Phys. Lett.* **85** 1045
[17] Xu T B and Su J 2005 *J. Appl. Phys.* **97** 034908
[18] Plante J S and Dubowsky S 2006 *Int. J. Solids Struct.* **43** 7727
[19] Patrick L, Gabor K and Silvain M 2007 *Sensors Actuators* A **135** 748
[20] Wissler M and Mazza E 2007 *Sensors Actuators* A **134** 494
[21] Mockensturm E M and Goulbourne N 2006 *Int. J. Non-Linear Mech.* **41** 388
[22] Goulbourne N C, Mockensturm E M and Frecker M I 2007 *Int. J. Solids Struct.* **44** 2609
[23] Arruda E M and Boyce M C 1993 *J. Mech. Phys. Solids* **41** 389
[24] Chater E and Hutchinson J W 1984 *J. Appl. Mech.* **51** 269
[25] Corona E and Kyriakides S 1998 *Int. J. Solids Struct.* **24** 505
[26] Kofoda G, Wirges W, Paajanen M and Bauer S 2007 *Appl. Phys. Lett.* **90** 081916
[27] Zhao X and Suo Z 2007 *Appl. Phys. Lett.* **91** 061921
[28] Zhao X, Hong W and Suo Z 2007 *Phys. Rev.* B **76** 134113
[29] Suo Z, Zhao X and Greene W H 2008 *J. Mech. Phys. Solids* **56** 476
[30] Zhou J, Hong W, Zhao X, Zhang Z and Suo Z 2008 *J. Solids Struct.* **45** 3739
[31] Zhao X and Suo Z 2008 *J. Appl. Phys.* **101** 123530
[32] Liu Y, Liu L, Zhang Z, Shi L and Leng J 2008 *Appl. Phys. Lett.* **93** 106101
[33] Norrisa A N 2007 *Appl. Phys. Lett.* **92** 026101
[34] Díaz-Calleja R, Riande E and Sanchis M J 2008 *Appl. Phys. Lett.* **93** 101902
[35] Kofod G, Sommer-Larsen P, Kronbluh R and Pelrine R 2000 *J. Intell. Mater. Syst. Struct.* **14** 787
[36] Liu Y, Liu L, Sun S, Shi L and Leng J 2009 *Appl. Phys. Lett.* **94** 096101
[37] Leng J, Liu L, Liu Y, Yu K and Sun S 2009 *Appl. Phys. Lett.* **94** 211901
[38] Liu Y, Liu L, Sun S and Leng J 2009 Stability analysis of dielectric elastomer film actuator *Sci. China* E at press
[39] Liu Y, Liu L, Leng J and Zhang Z 2009 Dielectric elastomer film actuator: characterization, experiments and analysis *Smart Mater. Struct.* **18** 095024